

Supporting Information

Moisture-inhibited deprotonation at the buried interface enables efficient perovskite solar cells with high fill factor over 86%

Shengwen Zou^a, Jingjing Zhang^a, Yi Xin^a, Jinlong Jin^a, Guangxin Liu^a, Xiaojun Yan^{abc}, Jianmei Huang^{*abc}

^aSchool of Energy and Power Engineering, Beihang University, Beijing 100191, China.

^bNational Key Laboratory of Science and Technology on Aero-Engine Aero-thermodynamics, Beihang University, Beijing, 100191, China.

^cBeijing Key Laboratory of Aero-Engine Structure and Strength, Beihang University, Beijing 100191, China.

*E-mail: jmhuang@buaa.edu.cn

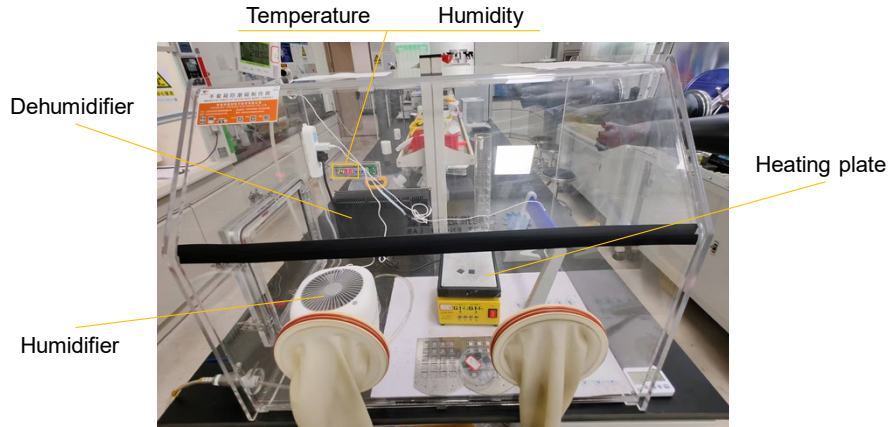


Figure S1. Photograph of the humidity-controlled glove box. The humidity control system contained a Dehumidifier and Humidifier. For the fabrication of Amb-PSCs, the humidity was controlled at $28\pm5\%$ RH by the synergistic operation of Dehumidifier and Humidifier. This glove box helps to create an artificial humidity-controlled atmosphere for devices fabrication according to requirements.

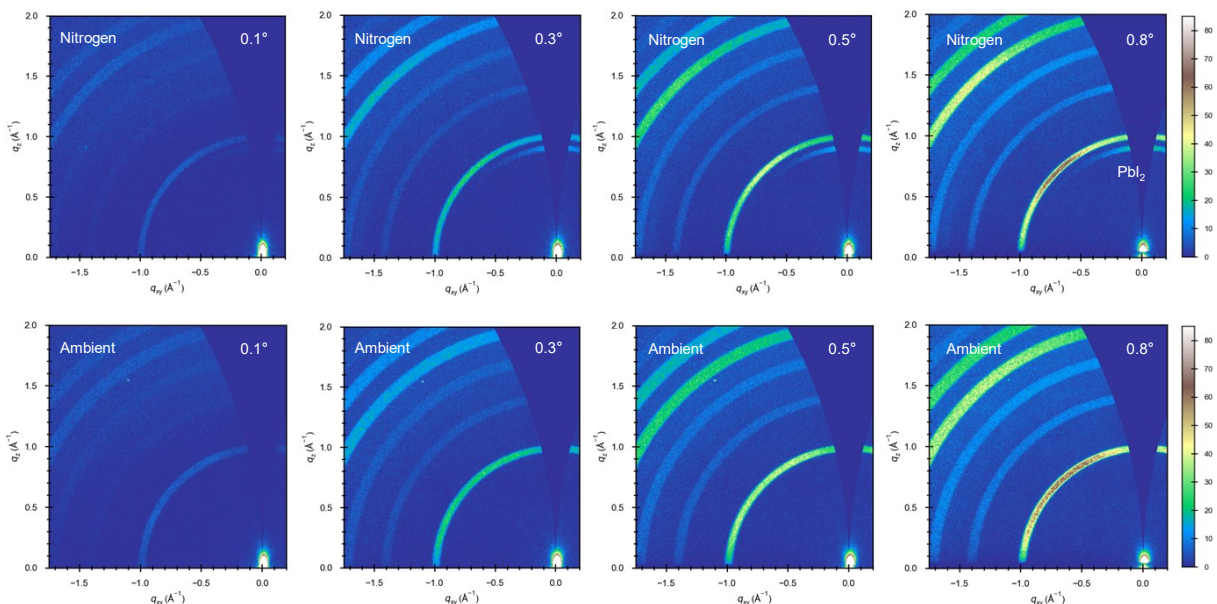


Figure S2. Depth-resolved GIWAXS patterns of the N_2 - and Amb-perovskite film with incident angles of 0.1° , 0.3° , 0.5° and 0.8° .

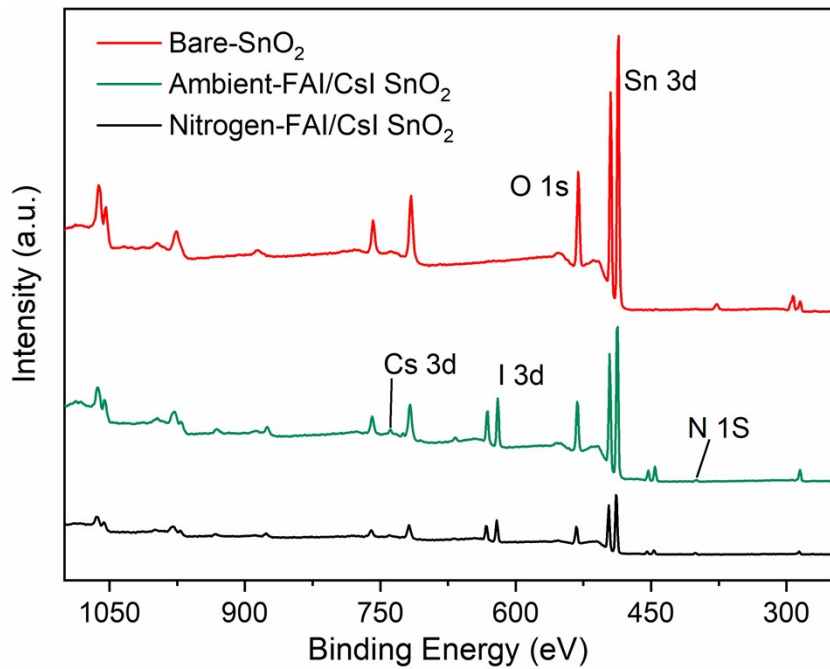


Figure S3. Survey XPS spectrum of the bare-SnO₂ film and FAI/CsI-deposited SnO₂ films.

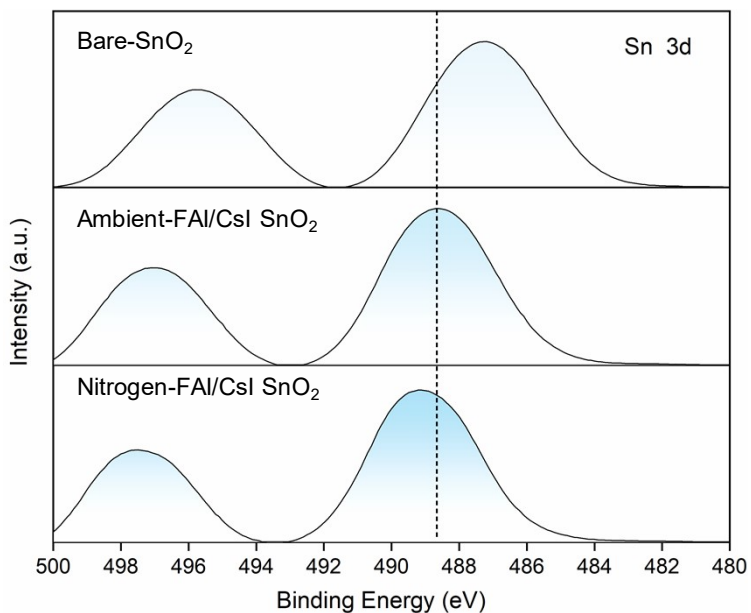


Figure S4. Sn 3d XPS spectra and fittings of the bare-SnO₂ film and FAI/CsI-deposited SnO₂ films.

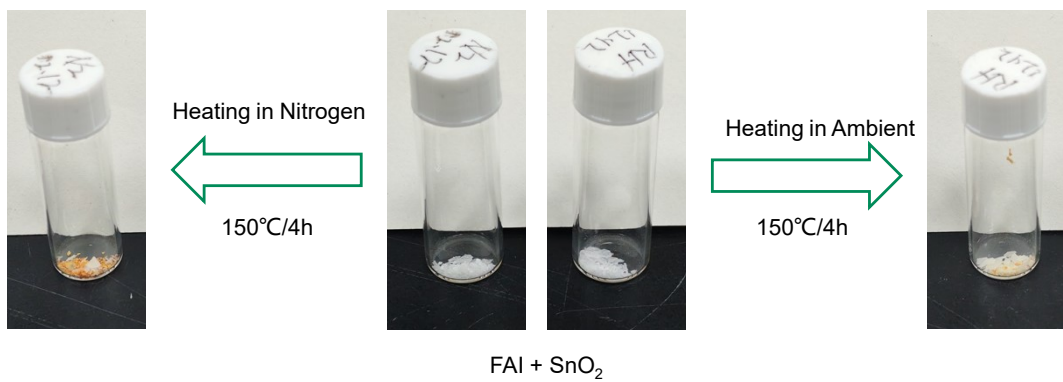


Figure S5. Digital photographs of the FAI/SnO₂ reaction. The mixtures of FAI and SnO₂ were heated at 150 °C for 4 h in Nitrogen or Ambient atmosphere. The bottle caps were opened during heating to ensure gas flow.

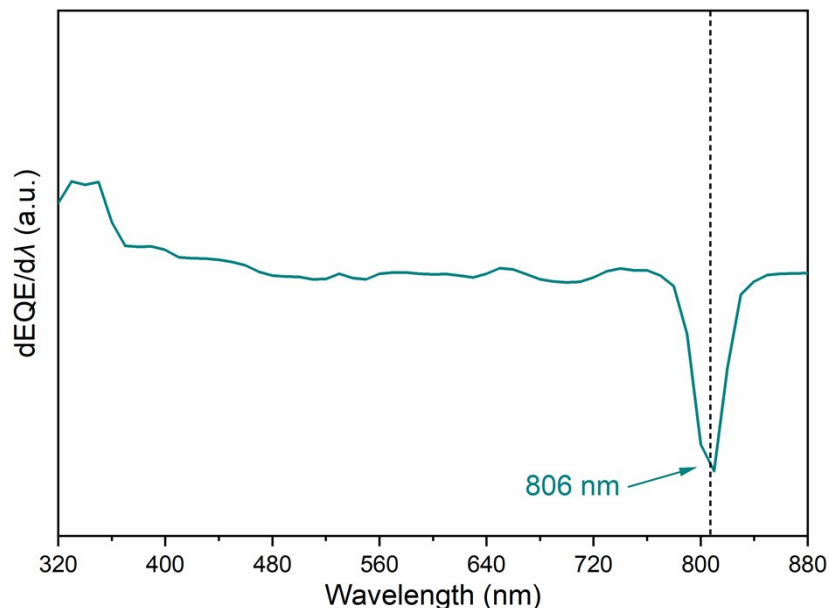


Figure S6. The plot of the first order derivative of EQE curve.

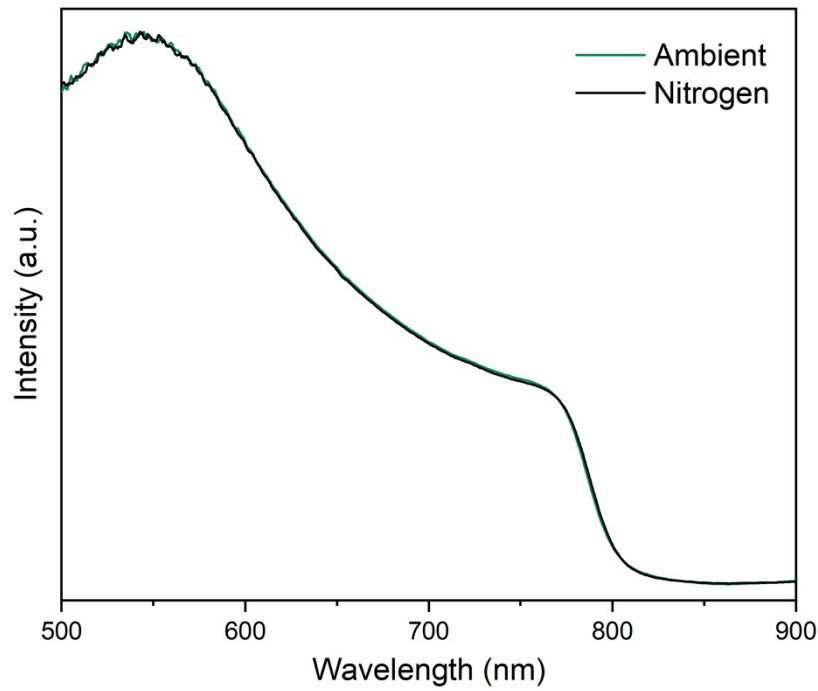


Figure S7. UV-vis absorption spectra of perovskite films annealed under nitrogen and ambient atmospheres.

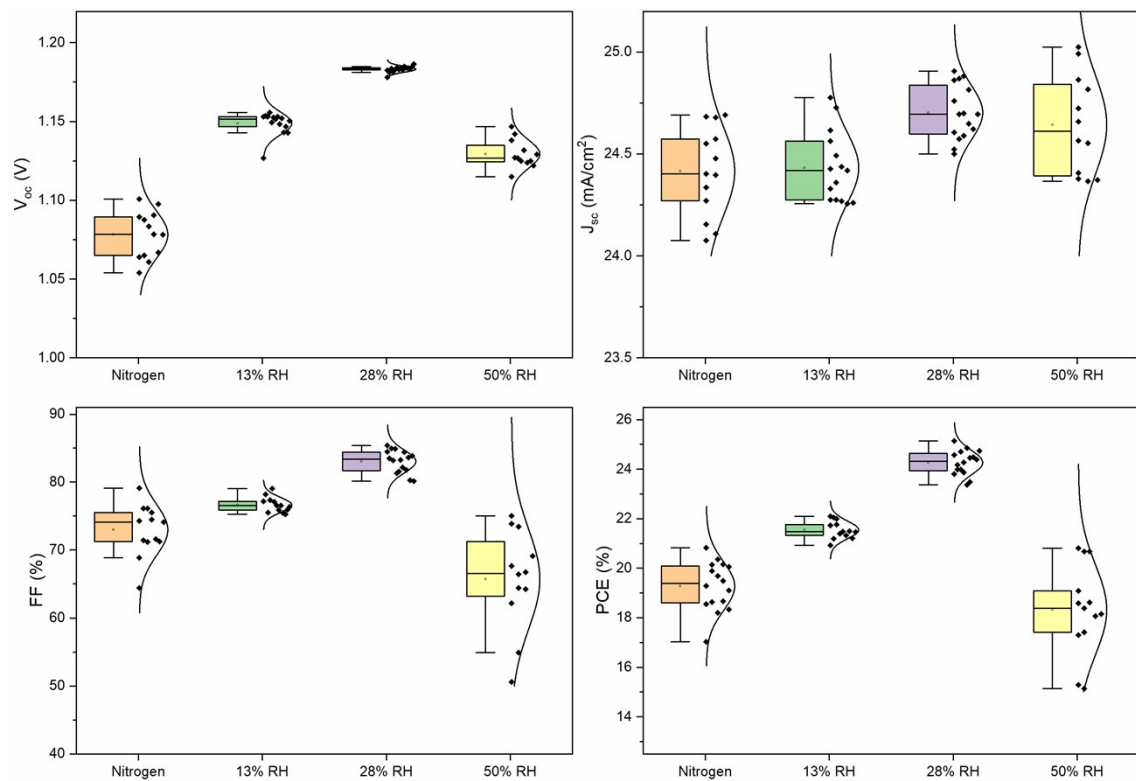


Figure S8. Photovoltaic parameters statistics of the N₂- and Amb-PSCs with 13% RH, 28% and 50%RH.

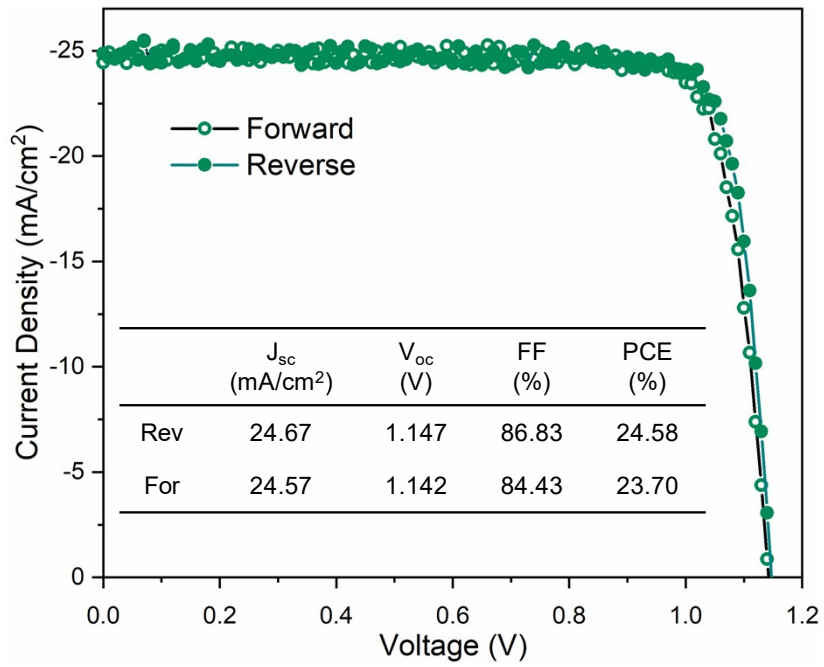


Figure S9. J-V curves of the highest FF (86.83%) device based on Amb-perovskite. The value of 86.83% has reached 96.3% of the S-Q limit FF (90.19% for the bandgap of 1.54 eV).

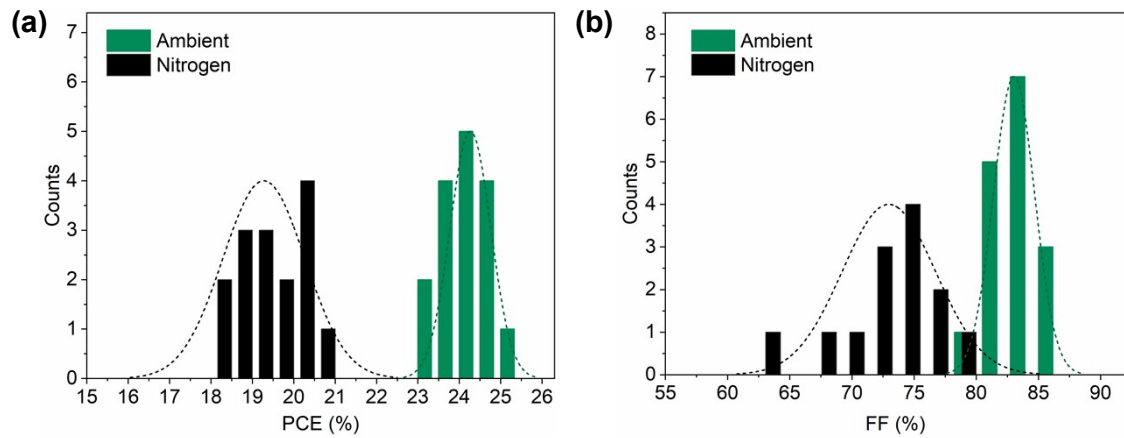


Figure S10. (a) PCE and (b) FF distribution of the 0.09 cm² PSCs.

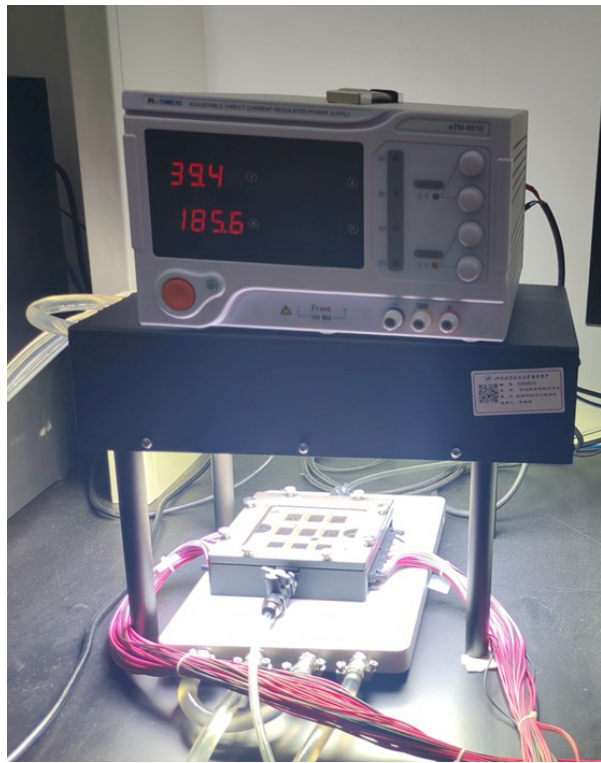


Figure S11. Photograph of the operational stability test setup.

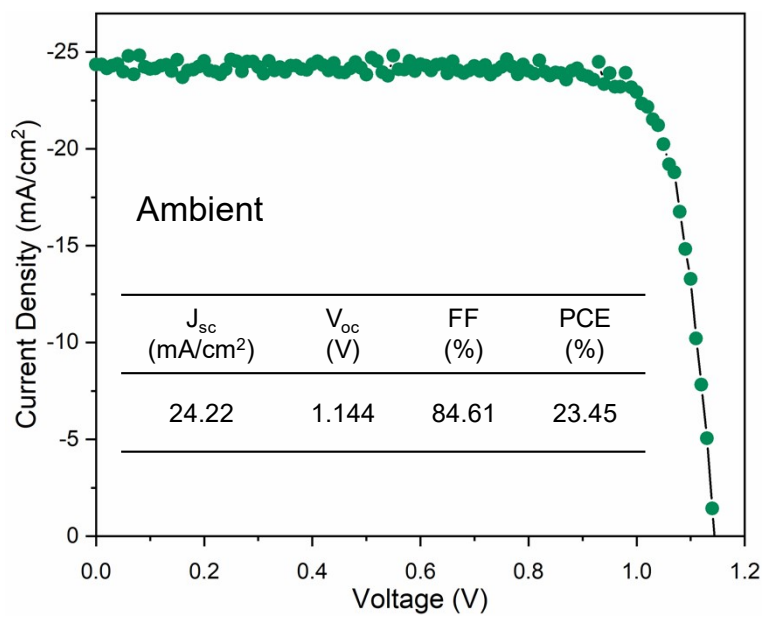


Figure S12. Initial efficiency of the Amb-PSC for MPPT stability test in **Figure 4j**.

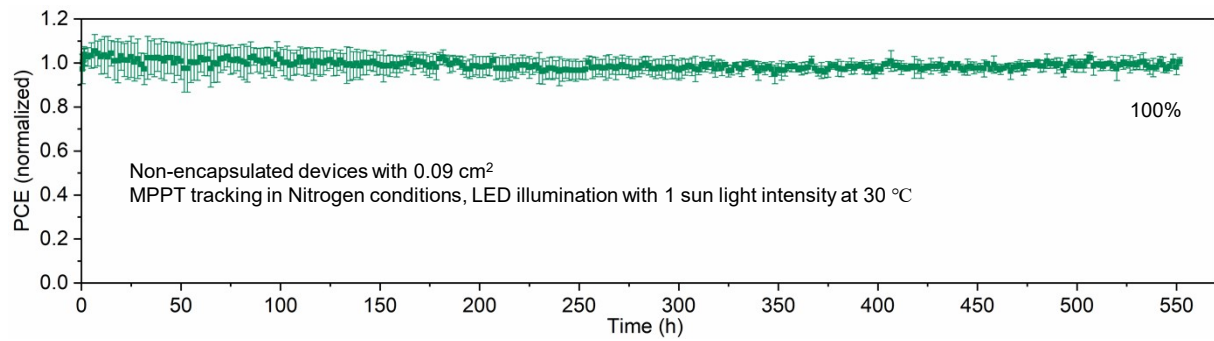


Figure S13. Operational stability of 4 independent Amb-PSCs under 1-sun illumination under nitrogen atmosphere at room temperature ($\sim 30^\circ\text{C}$). Data points and vertical line represent the average PCE and standard deviation, respectively.

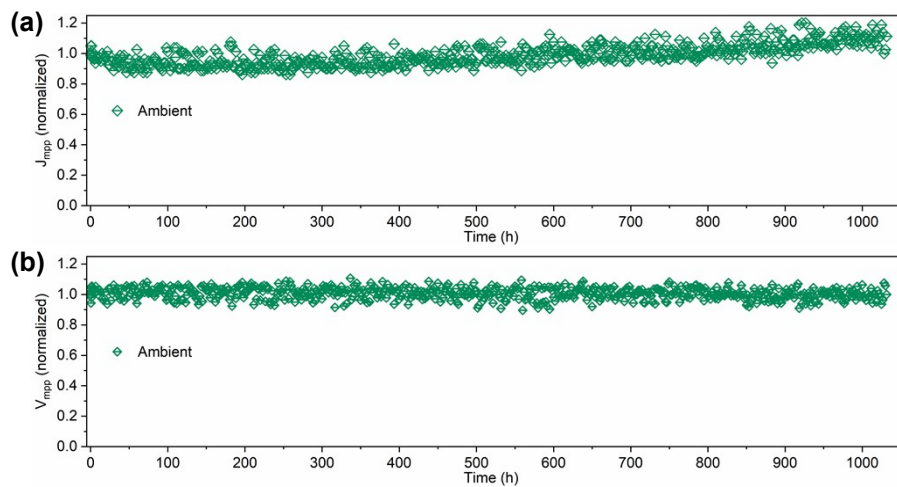


Figure S14. The evolution of voltage (a) and current (b) at the max power point (MPP) of the Amb-PSC that was shown in **Figure 4j**.

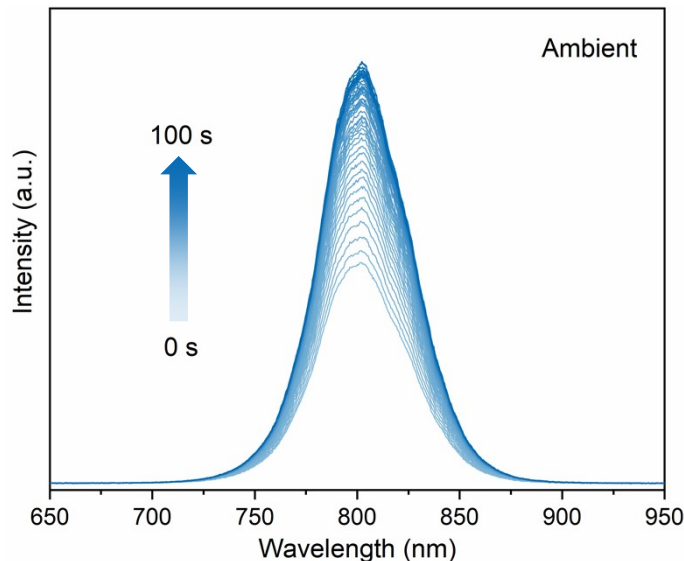


Figure S15. Steady-state PL spectra of the Ambient growth perovskite films over time illuminated by 420 nm laser. The PL intensity increased significantly over time, indicating trap density reduction after light illumination.

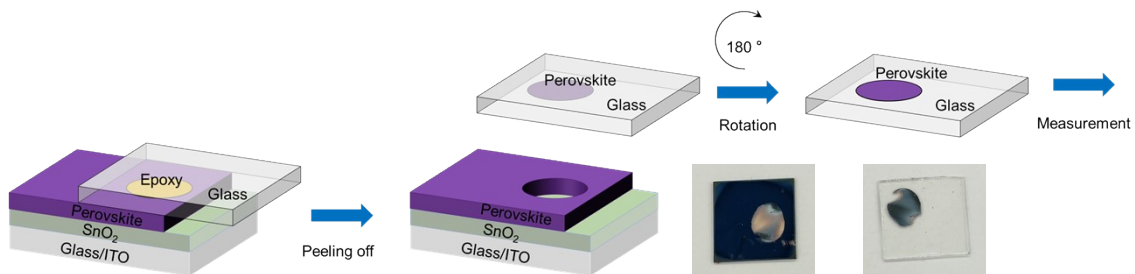


Figure S16. Schematic diagram of the exposing process for XRD measurements at buried interface.

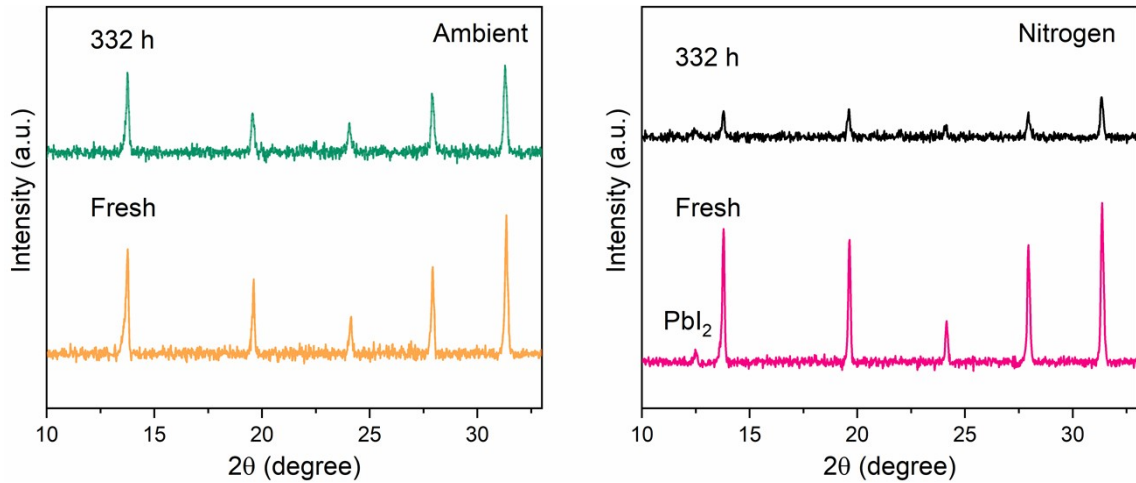


Figure S17. XRD patterns of buried interface of the Ambient grown perovskite film after aging under 1-sun illumination. There are almost no changes in XRD patterns of the Amb-perovskite after 164 h under 1-sun illumination, indicating the intrinsic stability.

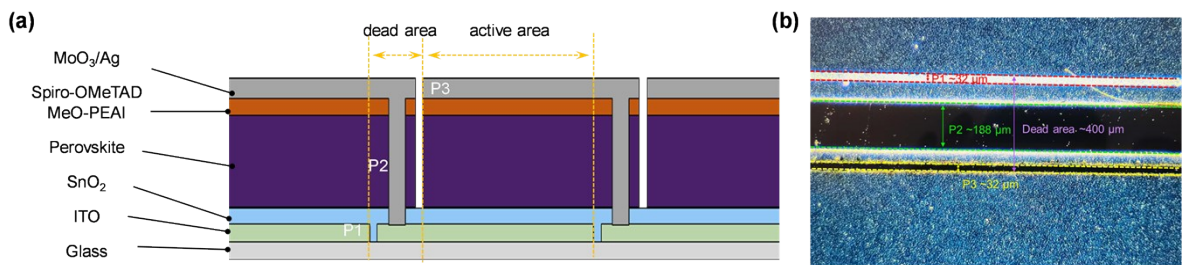


Figure S18. Design of the subcells. (a) section schematic diagram of the module, showing the P1, P2, P3 interconnections. (b) optical photograph of the P1-P2-P3 interconnections. Dead area width was $\sim 400 \mu\text{m}$, total width of the subcell was 5 mm, thereby the geometrical fill factor (GFF) was $\sim (5\text{mm}-0.4\text{mm})/5\text{mm}=92\%$.

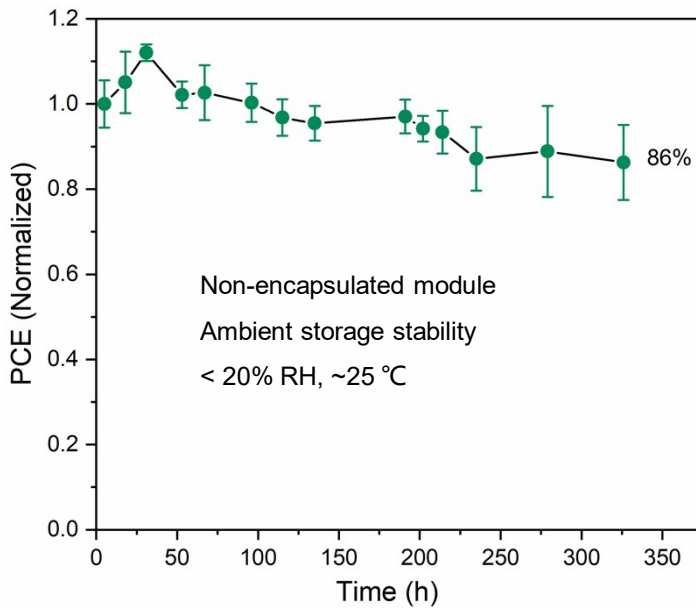


Figure S19. Storage stability of 4 independent Amb-PSC modules. Data points and vertical line represent the average PCE and standard deviation, respectively.

Table S1. Integral area percentages of $-\text{OH}$ and SnO to SnO_2 in Figure 2c.

Sample	$-\text{OH}/\text{SnO}_2$	SnO/SnO_2
Bare- SnO_2	66.7%	25.1%
Ambient-FAI/CsI SnO_2	56.7%	27.3%
Nitrogen-FAI/CsI SnO_2	41.9%	40.4%

Table S2. Fitting parameters of the TRPL decay curves of perovskite growth in nitrogen and ambient conditions.

Sample	τ_{ave} (ns)	τ_1 (ns)	A_1	τ_2 (ns)	A_2	τ_3 (ns)	A_3
Nitrogen	283.92	2.65	0.63	47.90	0.22	350.15	0.13
Ambient	357.27	4.26	0.53	65.08	0.26	435.30	0.17

Table S3. Comparison of FF and PCE of the champion Amb-PSC in this work with other reported FACs devices with PCE over 24%.

Component	V_{oc} (V)	J_{sc} (mA/cm ²)	FF (%)	PCE (%)	Ref.
FA _{0.9} Cs _{0.1} PbI ₃	1.191	25.27	81.88	24.64	1
FA _{0.95} Cs _{0.05} PbI ₃	1.164	26.14	85.74	26.09	2
FA _{0.9} Cs _{0.1} PbI ₃	1.17	25.67	85.3	25.7	3
FA _{0.9} Cs _{0.1} PbI ₃	1.2	25.21	83.48	25.24	4
FA _{0.9} Cs _{0.1} PbI ₃	1.2	25.11	82.75	24.96	5
FA/CsPbI ₃	1.175	26.47	84.94	26.41	6
FA _{0.91} Cs _{0.09} PbI ₃	1.18	25.28	83.00	24.7	7
FA _{0.98} Cs _{0.02} PbI ₃	1.176	25.88	82.50	25.1	8
FA _{0.9} Cs _{0.1} PbI ₃	1.166	25.55	86.21	25.69	This work

References

1. Z. Li, M. Wu, L. Yang, K. Guo, Y. Duan, Y. Li, K. He, Y. Xing, Z. Zhang, H. Zhou, D. Xu, J. Wang, H. Zou, D. Li and Z. Liu, *Adv. Funct. Mater.*, 2023, **33**, 2212606.
2. Z. Liang, Y. Zhang, H. Xu, W. Chen, B. Liu, J. Zhang, H. Zhang, Z. Wang, D.-H. Kang, J. Zeng, X. Gao, Q. Wang, H. Hu, H. Zhou, X. Cai, X. Tian, P. Reiss, B. Xu, T. Kirchartz, Z. Xiao, S. Dai, N.-G. Park, J. Ye and X. Pan, *Nature*, 2023, **642**, 557-563.
3. J. Li, H. Liang, C. Xiao, X. Jia, R. Guo, J. Chen, X. Guo, R. Luo, X. Wang, M. Li, M. Rossier, A. Hauser, F. Linardi, E. Alvianto, S. Liu, J. Feng and Y. Hou, *Nat. Energy*, 2024, **9**, 308-315.
4. L. Yang, H. Zhou, Y. Duan, M. Wu, K. He, Y. Li, D. Xu, H. Zou, S. Yang, Z. Fang, S. Liu and Z. Liu, *Adv. Mater.*, 2023, **35**, 2211545.
5. H. Zhou, L. Yang, Y. Duan, M. Wu, Y. Li, D. Xu, H. Zou, J. Wang, S. Yang and Z. Liu, *Adv. Energy Mater.*, 2023, **13**, 2204372.
6. J. Zhou, L. Tan, Y. Liu, H. Li, X. Liu, M. Li, S. Wang, Y. Zhang, C. Jiang, R. Hua, W. Tress, S. Meloni and C. Yi, *Joule*, 2024, 1691-1706.
7. H. Chen, Y. Wang, Y. Fan, Y. Chen, Y. Miao, Z. Qin, X. Wang, X. Liu, K. Zhu, F. Gao and Y. Zhao, *Natl. Sci. Rev.*, 2022, **9**, nwac127.
8. R. Chen, J. Wang, Z. Liu, F. Ren, S. Liu, J. Zhou, H. Wang, X. Meng, Z. Zhang, X. Guan, W. Liang, P. A. Troshin, Y. Qi, L. Han and W. Chen, *Nat. Energy*, 2023, **8**, 839-849.